Wave-packet-evolution approach for single and double ionization of two-electron systems by fast electrons

Vladislav V. Serov and Vladimir L. Derbov
Chair of Theoretical and Nuclear Physics, Saratov State University, 83 Astrakhanskaya, Saratov 410026, Russia

Boghos B. Joulakian
Laboratoire de Physique Moléculaire et des Collisions, Université Paul Verlaine, Metz, 1 Rue Arago, 57078 Metz Cedex 3, France

Sergue I. Vinitsky
Laboratory of Theoretical Physics, Joint Institute for Nuclear Research, Dubna 141980, Moscow Region, Russia
(Received 22 November 2006; published 22 January 2007)

We propose a method for direct calculation of the multiply differential cross section of the single and double ionization of two-electron atomic and molecular systems, which involves the reduction of the initial nine-dimensional Schrödinger equation to an evolution problem followed by the modeling of the wave packet dynamics. The cross section is obtained by the method of a time-scaled coordinate system. This approach, which describes well the behavior of two slow ejected electrons, avoids the use of rather uncertain cumbersome complex final-state functions of the continuous spectrum. Our results agree with those obtained by the convergent-close-coupling approach which is the object of some reserve because of ambiguity about its asymptotic behavior.

DOI: 10.1103/PhysRevA.75.012715 PACS number(s): 34.80.Dp, 32.80.Fb

I. INTRODUCTION

The study of the $(e,3e)$ reaction in atomic and molecular systems is the subject of many experimental works [1–4] as it provides valuable information about the electronic structure of the target and permits one to evaluate electron-electron correlation and other interactions. Discussions are going on [5–7] about the choice of the initial and final wave functions of the four-body Coulomb scattering problem. These discussions are stimulated by disagreement between the existing theoretical descriptions and experimental observations [1] in the $(e,3e)$ reaction with helium atoms. Different approaches have been used to calculate the fully differential cross section of the $(e,3e)$ reaction. Direct numerical calculations of this reaction using the convergent-close-coupling (CCC) method [5,8,9] for the final double-continuum state wave function of two slow ejected electrons lead to an underestimation of the magnitude of the cross section by several times. This disagreement stimulated some theoretical activity which tried to introduce some approximate analytical expressions for the final [6] and initial [7] wave functions satisfying some special conditions. Although a better fit between the calculated and measured cross sections was achieved, these approximate functions used can be hardly considered as satisfactory, since they poorly satisfy the initial Schrödinger equation. As a result, the use of these functions in the case of the parameters change or other phenomena (e.g., photoionization) considered yields in poor agreement with experiment.

There are several hypotheses that may explain the difficulties of the existing theory. First, it is possible that the Born expansion is principally inapplicable in the case of $(e,3e)$ for incident electron energy lower than several keV. Second, the reason may be that the wave functions of the initial and final states do not satisfy the cusp conditions in the vicinity of the collision point near the nucleus that mainly contributes to the proper matrix elements. Third, the observed difference may be due to the asymptotic behavior of the wave function of the two slow electrons at large distances from the nucleus, which is not taken into account by the CCC method. The aim of the present paper is to check the third hypothesis by taking into account the correct asymptotic behavior of the wave function of two slow electrons.

The solutions of this problem are known in double photoionization, where several numerical methods alternative to CCC have been successfully applied, such as the hyperspherical R-matrix approach with semiclassical outgoing wave (HRM-SOW)[10], and the external complex-scaling (ECS) [11], and the time-dependent close-coupling (TDCC) [12] methods. These methods account for the asymptotic behavior in a certain way. In the HRM-SOW method the asymptotic behavior of the three-body continuum states is taken into account by direct use of the quasiaclassical asymptotic functions. In the ECS method the extrapolation of the ionization flux to infinity is used for this purpose [13]. The difference between the CCC, ECS, and HRM-SOW methods in the case of asymmetric energy sharing is shown in [11,14]. Although in double photoionization the agreement between the methods mentioned above is good, there is no guarantee that it will be so for electron-impact double ionization.

In the present paper we reduce the initial stationary Schrödinger equation describing the interaction of a fast incident electron with a two-electron target to an evolution problem using approximation analogous to that of paraxial optics [15]. Then the modeling of the wave packet dynamics is carried out by means of the modified TDCC method using the time-dependent scaling (TDS) transformation [16–18]. The similarity of our approach to the TDCC method is that

we also use an expansion in the bispherical basis for angular variables and a finite-difference grid for radial ones to solve a Schrödinger-type equation. The difference is that (i) the very equation is modified due to time-dependent scaling and (ii) we use a different time propagation numerical scheme. The evolution approach removes the main difficulty in solving stationary problems with two electrons in the field of the nucleus that consists in imposing outgoing boundary condition [19]. Although the original TDCC method does not use the wave functions of the continuous spectrum of the two ejected electrons in solving the evolution problem, they are, however, necessary for extraction of the amplitudes by projecting the wave packet onto them [12]. The time-dependent scaling transformation allows one to calculate directly the multiply differential cross section of the single and double ionization of two-electron systems avoiding this projection procedure [18].

To implement the modified TDCC approach with time-dependent scaling we had to develop an original numerical scheme based on the split-operator method [20]. The discrete variable representation (DVR)[21] was used to diagonalize the electron-electron interaction. For efficient implementation of the DVR we propose a dynamical version of the Chang-Fano (CF) transformation [22] from a bispherical basis to a D basis and back.

In Sec. II we reduce the initial stationary problem to a lower-dimensional time-dependent Schrödinger equation. In Sec. III we describe the procedure of the extraction of the $(e,2e)$ and $(e,3e)$ cross sections from the resulting wave packet using the time-scaled space variable technique. In Sec. IV we present a numerical scheme for the solution of the evolution problem. In Sec. V the results of the calculations are discussed and compared with those of other authors.

II. PARAXIAL METHOD

Consider a general model of a molecule with N_{nuc} fixed nuclei and N electrons interacting with a single fast impact electron. This system is described by the $3(N+1)$-dimensional stationary Schrödinger equation

$$\left[H_0(\mathbf{r}) - \frac{1}{2}\nabla^2_{\mathbf{r}_0} + V(\mathbf{r},\mathbf{r}_0)\right]\Phi(\mathbf{r},\mathbf{r}_0) = (k_i^2/2 + E_0)\Phi(\mathbf{r},\mathbf{r}_0). \tag{1}$$

Here $\mathbf{r}=\{\mathbf{r}_\alpha\}_{\alpha=1}^N$ is the set of position vectors of the molecular electrons, $\hat{H}_0$ is the molecular Hamiltonian, $\mathbf{r}_0$ is the position vector of the fast impact electron, $V(\mathbf{r},\mathbf{r}_0)=U(\mathbf{r}_0)+U_{int}(\mathbf{r},\mathbf{r}_0)$ describes the interaction between the impact electron and the molecule, $U(\mathbf{r}_0)=-\Sigma_{\beta=1}^{N_{nuc}}Z_\beta/|\boldsymbol{\rho}_\beta-\mathbf{r}_0|$ is the potential of attraction between the incident electron and the nuclei, $U_{int}(\mathbf{r},\mathbf{r}_0)=\Sigma_{\alpha=1}^{N}1/|\mathbf{r}_\alpha-\mathbf{r}_0|$ is the potential of repulsion between the electrons, and E_0 is the energy of the target initial state having the wave function $\phi_0(\mathbf{r})$.

Let us seek the solution of Eq. (1) in the form $\Phi(\mathbf{r},x_0,y_0,z_0)=\psi(\mathbf{r},\mathbf{r}_{0\perp},z_0)\exp(ik_iz_0)$ [15]. By analogy with the paraxial approximation in beam optics one can neglect the second derivative of ψ with respect to the slow variable z_0. As a result we get an evolutionlike equation for the envelope function $\psi(\mathbf{r},\mathbf{r}_{0\perp},z_0)$:

$$ik_i\frac{\partial\psi(\mathbf{r},\mathbf{r}_{0\perp},z_0)}{\partial z_0} = \left\{\hat{H}_0(\mathbf{r}) - \frac{1}{2}\nabla^2_{\mathbf{r}_{0\perp}} - E_0 + V(\mathbf{r},\mathbf{r}_{0\perp},z_0)\right\}\psi(\mathbf{r},\mathbf{r}_{0\perp},z_0). \tag{2}$$

In the case of small scattering angles the initial condition for $\psi(\mathbf{r},\mathbf{r}_{0\perp},z_0)$ may be written as

$$\psi(\mathbf{r},\mathbf{r}_{0\perp},-\infty) = \phi_0(\mathbf{r}).$$

To solve the $(3N+2)$-dimensional Schrödinger evolution equation (2) we use the Fourier transformation of ψ with respect to $\mathbf{r}_{0\perp}$:

$$\psi(\mathbf{r},\mathbf{r}_{0\perp},z_0) = \frac{1}{2\pi}\int \tilde{\psi}_{\mathbf{k}_\perp}(\mathbf{r},z_0)\exp(-i\mathbf{k}_\perp\cdot\mathbf{r}_{0\perp})d\mathbf{k}_\perp.$$

The Fourier transform function $\tilde{\psi}_{\mathbf{k}_\perp}(\mathbf{r},z_0)$ satisfies the equation

$$ik_i\frac{\partial\tilde{\psi}_{\mathbf{k}_\perp}(\mathbf{r},z_0)}{\partial z_0} = \left\{\hat{H}_0(\mathbf{r}) + \left(\frac{k_\perp^2}{2} - E_0\right)\right\}\tilde{\psi}_{\mathbf{k}_\perp}(\mathbf{r},z_0) + \int V_{\mathbf{k}_\perp-\mathbf{k}'_\perp}(\mathbf{r},z_0)\tilde{\psi}_{\mathbf{k}'_\perp}(\mathbf{r},z_0)d\mathbf{k}'_\perp, \tag{3}$$

where

$$V_{\mathbf{k}_\perp}(\mathbf{r},z_0) = \frac{1}{(2\pi)^2}\int \exp(-i\mathbf{k}_\perp\cdot\mathbf{r}_{0\perp})V(\mathbf{r},\mathbf{r}_{0\perp},z_0)d\mathbf{r}_{0\perp} \tag{4}$$

is the Fourier transform of the interaction potential $V(\mathbf{r},\mathbf{r}_{0\perp},z_0)$.

Further simplification of the problem is possible if the amplitude of the incident wave is much greater than that of the scattered wave. In this case the approximation

$$\tilde{\psi}_{\mathbf{k}'_\perp}(\mathbf{r},z_0) \approx \delta(\mathbf{k}'_\perp)\psi_0(\mathbf{r})$$

may be applied, which is equivalent to keeping the first term only in the Born series [15]. Introducing the notation $t=z_0/k_i$ and $\tilde{\psi}_{\mathbf{k}_\perp}(\mathbf{r},k_it)=\psi_{\mathbf{k}_\perp}(\mathbf{r},t)\exp[-i(k_\perp^2/2-E_0)t]$ we get the Schrodinger-like inhomogeneous time-dependent equation

$$i\frac{\partial\psi_{\mathbf{k}_\perp}(\mathbf{r},t)}{\partial t} = \hat{H}_0(\mathbf{r})\psi_{\mathbf{k}_\perp}(\mathbf{r},t) + \exp\left[i\left(\frac{k_\perp^2}{2} - E_0\right)t\right]V_{\mathbf{k}_\perp}(\mathbf{r},k_it)\psi_0(\mathbf{r}), \tag{5}$$

with the initial condition $\psi_{\mathbf{k}_\perp}(\mathbf{r},-\infty)=0$, where $\mathbf{k}_\perp$ is the transverse component of the transferred momentum $\mathbf{K}$ [15] and

$$V_{\mathbf{k}_\perp}(\mathbf{r},z_0)=\frac{1}{2\pi k_\perp}\left[\sum_{\alpha=1}^{N} e^{-k_\perp|z_0-z_\alpha|+i\mathbf{k}_\perp\cdot\mathbf{r}_{\alpha\perp}} - \sum_{\beta=1}^{N_{nuc}} Z_\beta e^{-\frac{k_\perp}{\beta\perp}|z_0-\rho_{\beta z}|+i\mathbf{k}_\perp\cdot\boldsymbol{\rho}_{\beta\perp}}\right].$$

The latter expression follows from the inverse Fourier transformation of the Coulomb potential in momentum space with respect to the longitudinal momentum [15]. This potential vanishes exponentially as the impact time tends to zero. The transversal momentum transfer is given by $k_\perp \approx k_i \sin\theta_s$, where θ_s is the scattering angle.

III. IONIZATION DIFFERENTIAL CROSS SECTION

Our aim now is to extract the ionization amplitudes from the solution $\psi_{\mathbf{k}_\perp}(\mathbf{r},t)$. For simplicity let us start from a single-electron target with Coulomb potential and then proceed to a double-electron one. It is known [15] that the scattering amplitude $f(\mathbf{k}_e)$, $\mathbf{k}_e$ being the momentum of the ejected electron, can be expressed as

$$f(\Omega_s,E_e,\Omega_e)=-2\pi i k_i C(\mathbf{k}_e)$$

via the coefficients $C(\mathbf{k}_e)$ of the expansion of the solution $\psi(\mathbf{r},t)$ of Eq. (5) after the impact

$$\psi(\mathbf{r},t)=\int C(\mathbf{k})\phi_{\mathbf{k}}^{(-)}(\mathbf{r})e^{-iEt}d\mathbf{k}+\sum_{nlm} C_{nlm}\phi_{nlm}(\mathbf{r})e^{-iE_{nlm}t}. \tag{6}$$

Here $E=k^2/2$, $\phi_{\mathbf{k}}(\mathbf{r})$ are the continuum wave functions of the target normalized as

$$\int \phi_{\mathbf{k}'}^{(-)}(\mathbf{r})\phi_{\mathbf{k}}^{(-)}(\mathbf{r})d\mathbf{r}=\delta(\mathbf{k}'-\mathbf{k}),$$

and $\phi_{nlm}(\mathbf{r})$ are the bound-state functions of the target. According to [23], the asymptotic form of the solution is

$$\psi(\mathbf{r}\to\infty,t\to\infty)=\frac{1}{(it)^{3/2}}\exp\left(\frac{i}{2}\frac{r^2}{t}+i\frac{Z}{k_e}\ln 2k_e^2 t\right)C(\mathbf{k}_0), \tag{7}$$

where $\mathbf{k}_0$ represents the stationary point of the integral in Eq. (6),

$$\mathbf{k}_0=\mathbf{k}_e-Z\frac{\ln 2k_e^2 t}{k_e^2 t}\frac{\mathbf{k}_e}{k_e},$$

and $\mathbf{k}_e=\mathbf{r}/t$ is the electron momentum at large distances; here, Z is the charge of the residual ion.

Numerical representation of $\psi(\mathbf{r},t)$ faces problems related to the finite size of the spatial grid. When the wave packet propagates during a long time t, the continuum component of the wave function expands and is reflected from the finite grid boundary. Moreover, the spatial phase gradient increases with time, so that the wave function becomes strongly oscillating. To avoid these difficulties we apply the time-dependent scaling transformation [16,17]

$$\mathbf{r}=a(t)\boldsymbol{\xi}, \tag{8}$$

where $\boldsymbol{\xi}$ is the vector of projective coordinates and $a=a(t)$ is the scaling factor that depends only on time. Physically, this transformation makes the coordinates expand together with the continuum components of the wave function. The substitution of Eq. (8) into the time-dependent Schrödinger equation yields the following relation [17]:

$$\psi(\mathbf{r},t)=\frac{1}{a^{3/2}}\exp\left(\frac{i}{2}a\dot{a}\xi^2\right)\Psi(\boldsymbol{\xi},t), \tag{9}$$

where $\dot{a}=\frac{da}{dt}$ and $\Psi(\boldsymbol{\xi},t)$ is the "pilot wave function" of the solution $\psi(\mathbf{r},t)$ that satisfies the time-dependent Schrödinger-like equation [16]

$$i\frac{\partial}{\partial t}\Psi(\boldsymbol{\xi},t)=\left[\hat{H}_0(a(t)\boldsymbol{\xi})+\frac{1}{2}a(t)\ddot{a}(t)\xi^2\right]\Psi(\boldsymbol{\xi},t). \tag{10}$$

If $\ddot{a}>0$, the spectrum of the operator in the square brackets is purely discrete. This provides smooth behavior of the pilot solution $\Psi(\boldsymbol{\xi},t)$, and ensures normalization in the reduced interval $0\leqslant\xi\leqslant\xi_{max}$.

Consider the scale parameter increasing linearly in the asymptotic region:

$$a(t\to\infty)=\dot{a}_\infty t,\quad \dot{a}_\infty>0.$$

Comparing Eqs. (7) and (9), we arrive at the asymptotic definition of the envelope function at large t [18]:

$$\Psi(\boldsymbol{\xi},t)=(-i\dot{a}_\infty)^{3/2}C(\mathbf{k}_0)\exp\left(i\frac{Z}{k_e}\ln 2k_e^2 t\right),$$

where it is assumed that $\mathbf{k}_e=\dot{a}\boldsymbol{\xi}$. For finite t and $\xi\gg R_b/a$, where R_b is the typical radius of the excited bound states, we get

$$|C(\mathbf{k}_e)|^2=\frac{1}{\dot{a}_\infty^3}|\Psi(\mathbf{k}_e/\dot{a}_\infty,t)|^2+O(Z\ln t/t)+O(R_i/t), \tag{11}$$

where R_i is the radius of the wave packet before the expansion.

Finally, the triple-differential ionization cross section, describing the ejection of the initially bound electron that finally gets the given momentum $\mathbf{k}_e$ by the projectile electron with the initial momentum $\mathbf{k}_i$, may be expressed as

$$\sigma^{(3)}(\Omega_s,E_e,\Omega_e)=4\pi^2 k_i k_s k_e \dot{a}_\infty^{-3}\lim_{t\to\infty}|\Psi(\mathbf{k}_e/\dot{a}_\infty,t)|^2.$$

Now let us consider a two-electron target. For single ionization, when one of the electrons stays near the nucleus in the ion bound state (n,l,m), the cross section takes the form

$$\sigma^{(3)}(\Omega_s,E_2,\Omega_2)=4\pi^2 k_i k_s k_2 \dot{a}_\infty^{-3}\lim_{t\to\infty}a^{3/2}(t) \times|\langle\phi_{nlm}(a(t)\boldsymbol{\xi}_1)|\Psi(\boldsymbol{\xi}_1,\mathbf{k}_2/\dot{a}_\infty,t)\rangle|^2,$$

while for double ionization,

$$\sigma^{(5)}(\Omega_s,E_1,\Omega_1,E_2,\Omega_2) =4\pi^2 k_i k_s k_1 k_2 \dot{a}_\infty^{-6}\lim_{t\to\infty}|\Psi(\mathbf{k}_1/\dot{a}_\infty,\mathbf{k}_2/\dot{a}_\infty,t)|^2.$$

For single-photon photoionization Kazansky *et al.* [19] have shown how to derive the cross section directly by solving the time-dependent Schrödinger equation. Implementation of this approach is straightforward in the case of our numerical scheme and time-dependent scaling method for extraction of amplitudes. We solve Eq. (10) with the initial condition

$$\Psi(\mathbf{r}_1,\mathbf{r}_2,0) = (\mathbf{e}\cdot\mathbf{r}_1 + \mathbf{e}\cdot\mathbf{r}_2)\psi_0(\mathbf{r}_1,\mathbf{r}_2)$$

and get the cross section of one-photon photoionization in the coordinate gauge. For photons having energy E_γ the cross section is given by

$$\sigma^{(1)}_{E_\gamma}(\Omega_2) = \frac{4\pi^2 E_\gamma}{c} k_2 \dot{a}_\infty^{-3} \lim_{t\to\infty} a^{3/2}(t) \times |\langle \phi_{nlm}(a(t)\boldsymbol{\xi}_1)|\Psi(\boldsymbol{\xi}_1,\mathbf{k}_2/\dot{a}_\infty,t)\rangle|^2$$

for single photoionization and

$$\sigma^{(3)}_{E_\gamma}(\Omega_1,E_2,\Omega_2) = \frac{4\pi^2 E_\gamma}{c} k_1 k_2 \dot{a}_\infty^{-6} \lim_{t\to\infty} |\Psi(\mathbf{k}_1/\dot{a}_\infty,\mathbf{k}_2/\dot{a}_\infty,t)|^2$$

for double photoionization.

IV. NUMERICAL METHOD FOR THE HELIUM ATOM

Now let us consider a heliumlike atom and make use of both the paraxial approximation and the time-dependent scaling method. The appropriate two-electron Schrödinger-like inhomogeneous equation takes the form

$$i\frac{\partial\Psi(\boldsymbol{\xi}_1,\boldsymbol{\xi}_2,t)}{\partial t} = \{\hat{H}_1(t) + \hat{H}_2(t) + U(|\boldsymbol{\xi}_2 - \boldsymbol{\xi}_1|,t)\}\Psi(\boldsymbol{\xi}_1,\boldsymbol{\xi}_2,t) + F(\boldsymbol{\xi}_1,\boldsymbol{\xi}_2,t). \tag{12}$$

Here $\hat{H}_{1,2}(t)$ are one-electron Hamiltonians,

$$\hat{H}_\alpha(t) = -\frac{1}{2a^2(t)}\nabla^2_{\xi_\alpha} - \frac{Z}{a(t)\xi_\alpha} + \frac{a(t)\ddot{a}(t)}{2}\xi^2_\alpha,$$

and $U(\xi_{12},t)$ is the potential of electron-electron interaction,

$$U(\xi_{12},t) = \frac{1}{a(t)\xi_{12}}.$$

The term $F(\boldsymbol{\xi}_1,\boldsymbol{\xi}_2,t)$ on the right-hand side is the source term of Eq. (5) in projective coordinates.

After the impact the full angular momentum and its projection are conserved; hence, the solution may be presented as

$$\Psi(\boldsymbol{\xi}_1,\boldsymbol{\xi}_2,t) = \sum_{LM}\Psi^{LM}(\boldsymbol{\xi}_1,\boldsymbol{\xi}_2,t), \tag{13}$$

where L and M are the quantum numbers of the full angular momentum and its projection, respectively. We expand Ψ^{LM} in terms of bispherical harmonics [24]:

$$\Psi^{LM}(\boldsymbol{\xi}_1,\boldsymbol{\xi}_2,t) = \frac{1}{\xi_1\xi_2}\sum_{l_1,l_2} Y^{LM}_{l_1l_2}(\theta_1,\varphi_1,\theta_2,\varphi_2)\psi^{LM}_{l_1l_2}(\xi_1,\xi_2,t). \tag{14}$$

The coefficients of the analogous expansion of the source term $F(\boldsymbol{\xi}_1,\boldsymbol{\xi}_2,t)$ are denoted by

$$f^{LM}_{l_1l_2}(\xi_1,\xi_2,t) = \xi_1\xi_2\langle LMl_1l_2|F(\boldsymbol{\xi}_1,\boldsymbol{\xi}_2,t)\rangle.$$

To solve the resulting set of equations we use the split-operator method [20] in which each evolution step is split into substeps easily implemented by means of the simple Crank-Nicholson scheme. Introducing the radial grid $\{\xi_{1i_1},\xi_{2i_2}\}$, $i_\alpha = 1,\ldots,N_r$, the discrete time points t_n, and the notation $\psi^{LM}_{l_1l_2i_1i_2n} = \psi^{LM}_{l_1l_2}(\xi_{1i_1},\xi_{2i_2},t_n)$, the evolution from t_n to t_{n+2} can be accomplished by the following scheme:

$$\psi^{LM}_{l_1l_2i_1i_2n+1/4} = \psi^{LM}_{l_1l_2i_1i_2n} - i\tau_n f^{LM}_{l_1l_2i_1i_2n}, \tag{15a}$$

$$\left[\delta^j_{i_1} + \frac{i\tau_n}{2}\mathcal{H}^{j_1}_{l_1i_1}(t_{n+1})\right]\psi^{LM}_{l_1l_2j_1i_2n+1/2} = \left[\delta^j_{i_1} - \frac{i\tau_n}{2}\mathcal{H}^{j_1}_{l_1i_1}(t_{n+1})\right]\psi^{LM}_{l_1l_2j_1i_2n+1/4}, \tag{15b}$$

$$\left[\delta^j_{i_2} + \frac{i\tau_n}{2}\mathcal{H}^{j_2}_{l_2i_2}(t_{n+1})\right]\psi^{LM}_{l_1l_2i_1j_2n+3/4} = \left[\delta^j_{i_2} - \frac{i\tau_n}{2}\mathcal{H}^{j_2}_{l_2i_2}(t_{n+1})\right]\psi^{LM}_{l_1l_2i_1j_2n+1/2}, \tag{15c}$$

$$\phi^{LM}_{km_2i_1i_2n+3/4} = \mathcal{P}^{l_2}_{km_2}\mathcal{C}^{Ll_1}_{l_2m_2}\psi^{LM}_{l_1l_2i_1i_2n+3/4}, \tag{15d}$$

$$\phi^{LM}_{kmi_1i_2n+5/4} = \frac{1 - i\tau_n U_{i_1i_2k}(t_{n+1})}{1 + i\tau_n U_{i_1i_2k}(t_{n+1})}\phi^{LM}_{kmi_1i_2n+3/4}, \tag{15e}$$

$$\psi^{LM}_{l_1l_2i_1i_2n+5/4} = \bar{\mathcal{C}}^{Lm_2}_{l_1l_2}\bar{\mathcal{P}}^{k}_{l_2m_2}\phi^{LM}_{km_2i_1i_2n+5/4}, \tag{15f}$$

$$\left[\delta^j_{i_2} + \frac{i\tau_n}{2}\mathcal{H}^{j_2}_{l_2i_2}(t_{n+1})\right]\psi^{LM}_{l_1l_2i_1j_2n+3/2} = \left[\delta^j_{i_2} - \frac{i\tau_n}{2}\mathcal{H}^{j_2}_{l_2i_2}(t_{n+1})\right]\psi^{LM}_{l_1l_2i_1j_2n+5/4}, \tag{15g}$$

$$\left[\delta^j_{i_1} + \frac{i\tau_n}{2}\mathcal{H}^{j_1}_{l_1i_1}(t_{n+1})\right]\psi^{LM}_{l_1l_2j_1i_2n+7/4} = \left[\delta^j_{i_1} - \frac{i\tau_n}{2}\mathcal{H}^{j_1}_{l_1i_1}(t_{n+1})\right]\psi^{LM}_{l_1l_2j_1i_2n+3/2}, \tag{15h}$$

$$\psi^{LM}_{l_1l_2i_1i_2n+2} = \psi^{LM}_{l_1l_2i_1i_2n+7/4} - i\tau_n f^{LM}_{l_1l_2i_1i_2n+2}. \tag{15i}$$

Here we follow the Einstein summation rule. Each time step $\tau_n = (t_{n+2} - t_n)/2$ is attributed to the mean time $t_{n+1} = (t_{n+2} + t_n)/2$. The matrices $\mathcal{H}^{j_\alpha}_{l'^{i_\alpha}_\alpha}(t)$ are finite-difference approximations of one-dimensional radial Hamiltonians

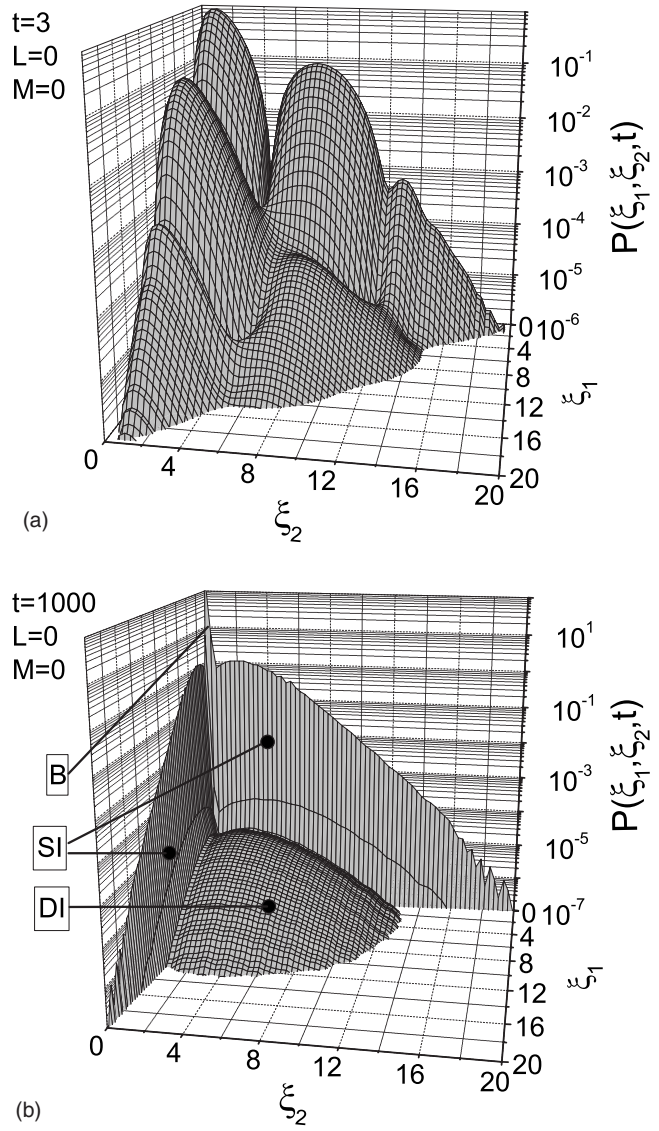

FIG. 1. The probability density integrated over the angular variables for $L=0$, $M=0$ versus the radial coordinates ξ_1, ξ_2 of two electrons: (a) after impact but before the start of expanding of coordinates ($t=3$ a.u.) and (b) within the space of expansion ($t=1000$).

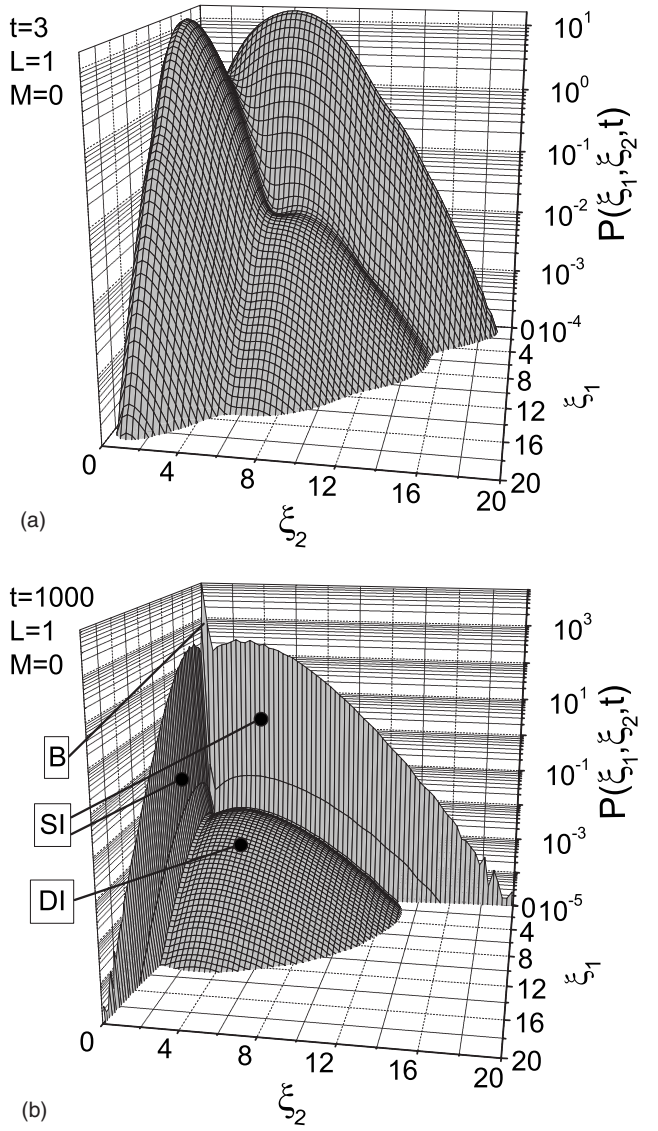

FIG. 2. The same as in Fig. 1 but for $L=1$, $M=0$.

$$\hat{H}_{\alpha l_\alpha}(t) = -\frac{1}{2a^2}\left(\frac{\partial^2}{\partial \xi_\alpha^2} - \frac{l_\alpha(l_\alpha+1)}{\xi_\alpha^2}\right) - \frac{Z}{a\xi_\alpha} + \frac{a\ddot{a}}{2}\xi_\alpha^2.$$

To diagonalize the electron-electron interaction we use two orthogonal transformations. First, the Chang-Fano transformation [22] is used to provide the conversion from the bispherical basis (14) to D basis [24]:

$$\Psi^{LM}(\boldsymbol{\xi}_1,\boldsymbol{\xi}_2,t) = \frac{1}{\xi_1\xi_2}\sqrt{\frac{2L+1}{4\pi}}\sum_{l_2,m_2} D^{L*}_{Mm_2}(\varphi_1,\theta_1,\varphi_{12}) \times Y_{l_2m_2}(\theta_{12},0)\chi^{LM}_{l_2m_2}(\xi_1,\xi_2,t), \quad (16)$$

where $D^l_{m_1m_2}$ is the Wigner function. The $[2\min(L,l_2)+1]\times[2\min(L,l_2)+1]$ matrices of the direct and inverse Chang-Fano transformations have the form

$$C^{Ll_1}_{l_2m_2} = (-1)^{l_2+m_2}C^{l_10}_{l_2-m_2Lm_2}, \quad (17a)$$

$$\bar{C}^{Lm_2}_{l_1l_2} = (-1)^{l_2+m_2}C^{l_10}_{l_2-m_2Lm_2}, \quad (17b)$$

where $C^{l_3m_3}_{l_1m_1l_2m_2}$ are the Clebsh-Gordan coefficients [24], $l_2=0,\ldots,l_{2\,max}$, $l_1=|L-l_2|,\ldots,L+l_2$, $m_2=-\min(L,l_2),\ldots,\min(L,l_2)$. For final diagonalization we use the discrete variable representation [21] based on the transformation

$$\phi^{LM}_{km}(\xi_1,\xi_2,t) = \sum_{l=0}^{N_m-1}\chi^{LM}_{lm}(\xi_1,\xi_2,t)P^m_l(\eta^m_k), \quad (18)$$

where $\phi^{LM}_{km}(\xi_1,\xi_2,t)$ is the value of the wave function in the kth node of the angular grid, $\eta=\cos\theta_{12}$, $\eta^{m_2}_k$ and $\lambda^{m_2}_k$ are the nodes and weights of corresponding Gauss-Legendre quadratures, $k=1,\ldots,N_{m_2}$, $P^m_l(\eta)$ are the normalized associated Legendre polynomials, and N_{m_2} is the number of the involved polynomials for given m_2. The matrices of dimen-

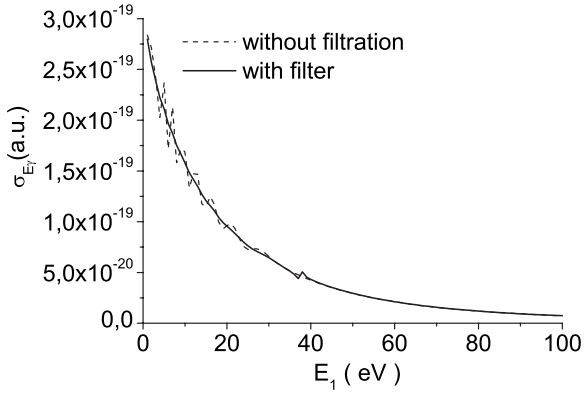

FIG. 3. Single-photoionization cross section versus the energy of the ejected electron, $E_1=E_\gamma+E_0$, calculated without filtration (dashed line), with linear and exponential filter (solid line).

sions $N_{m_2}\times N_{m_2}$ of direct and inverse transformations are

$$\mathcal{P}^l_{km} = P^m_l(\eta^m_k), \tag{19a}$$

$$\bar{\mathcal{P}}^k_{lm} = P^m_l(\eta^m_k)\lambda_k. \tag{19b}$$

The direct transformations are performed at step (15d) of the algorithm. The potential of an electron-electron interaction appears in the diagonal form as a function of the radial coordinates of two electrons and the angle θ_{12} between their radius vectors. As a result implementation of the Crank-Nicholson scheme (15e) is reduced to multiplication by the phase factor. Then the inverse transformations (15f) are performed to return to the bispherical basis convenient for calculations involving one-electron Hamiltonians. This procedure is particularly efficient in our case of a time-dependent grid, since the commonly used nondiagonal matrix representation $\langle l_1 l_2|U|l_1' l_2'\rangle$ of the electron-electron potential requires full matrix inversion for each node of the radial grid at each time step.

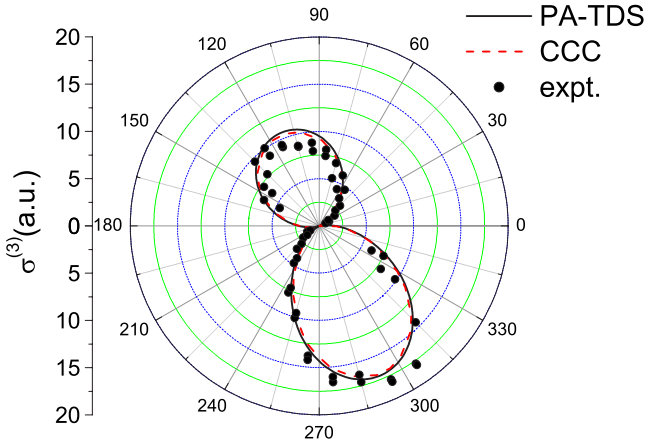

FIG. 4. (Color online) Single-ionization triple-differential cross section versus the ejection angle for the energy of impact electron, E_i=5600 eV; the scattering angle θ_s=0.45; and the energy of ejected electron, $E_{1,2}$=10 eV.

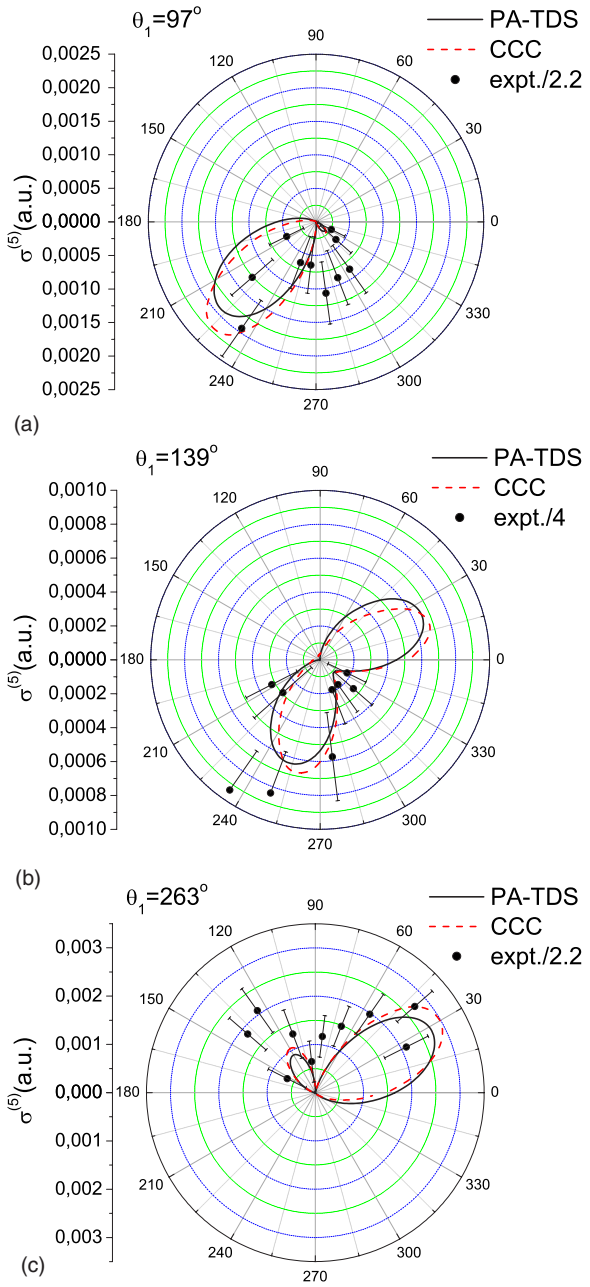

FIG. 5. (Color online) Coplanar double-ionization fivefold differential cross section versus θ_2 for the energy of the impact electron, E_i=5600 eV; the scattering angle θ_s=0.45; and energy of the ejected electrons, $E_1=E_2$=10 eV. The ejection angles are (a) θ_1 =97°, (b) θ_1=139°, and (c) θ_1=263°.

To implement the fourth-order finite-difference approximation of the second radial derivatives we choose a nonuniform radial grid with the nodes

$$\xi_{\alpha i} = b \tan s_{\alpha i}, \quad s_i = \frac{s_{max}}{N_r} i, \quad i = 1 \ldots N_r,$$

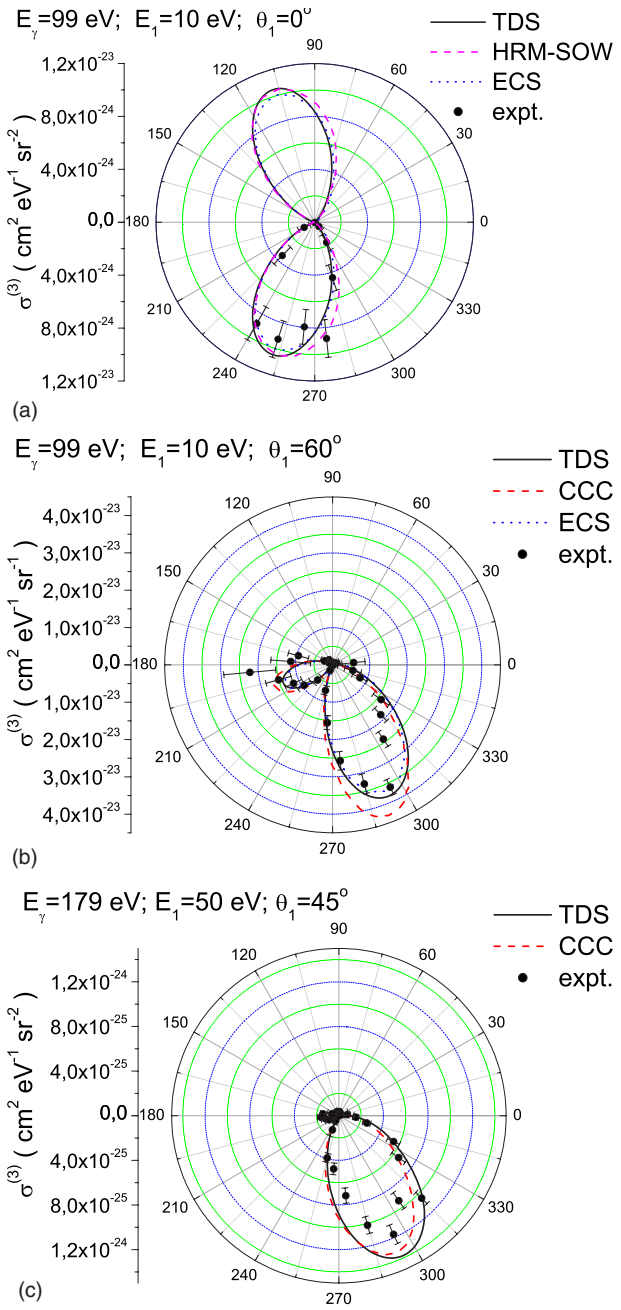

FIG. 6. (Color online) Double-photoionization threefold differential cross section versus θ_2 for fixed ejection angle θ_1 and equal energy sharing $E_1=E_2$. (a) $E_\gamma=99$ eV, $E_1=10$ eV, $\theta_1=0°$; (b) $E_\gamma=99$ eV, $E_1=10$ eV, $\theta_1=60°$; and (c) $E_\gamma=179$ eV, $E_1=50$ eV, $\theta_1=45°$.

$$b=\frac{r_u}{s_{max}},\quad \tan s_{max}=\frac{r_{max}}{r_u}s_{max},$$

where r_{max} is the size of the radial box, N_r is the number of nodes, and r_u is the grid parameter. In the vicinity of zero the step $h=\xi_{\alpha 1}-\xi_{\alpha 0}\approx r_u/N_r$. We constructed the finite-difference operator on this grid to be self-adjoint, which assures the Hermicity of the total Hamiltonian.

The source term is actual during the impact of the incident electron and exhibits an exponential decrease at large $|t|$. Hence the zero initial condition is imposed at the initial time $t=-t_{int}$. In the interval $[-t_{int},t_{int}]$ the source term is taken into account. At $t=t_{int}$ the negligible source term is omitted to decrease computational efforts. The time-dependent scaling factor is chosen in the form

$$a(t)=\begin{cases}1, & t\leqslant t_{int},\\ [1+\gamma^2(t-t_{int})^2]^{1/2}, & t>t_{int},\end{cases}$$

providing $\dot{a}_\infty=\gamma$.

In the calculations discussed below the parameters of the numerical scheme were chosen as $N_r=200$, $r_{max}=20$, $r_u=10$, $l_{2\ max}=11$, $t_{int}=3$, and $\gamma=0.5$.

The split-operator method is stable if the time step τ satisfies the condition

$$\tau\leqslant\frac{h^2}{4a^2}. \tag{20}$$

However, practical calculations show that for $L>0$ the step τ can be taken a few times larger without any harm. This fact is due to the absence of three-body collisions in the case $L>0$. We choose $\tau_n=\tau(t_{n+1})=a(t_{n+1})\tau_0$ because the Coulomb potential decreases as $1/a(t)$. Then the computer time needed to calculate the evolution up to given t is proportional to $\ln t$. In the present calculations we use the time step $\tau_0=h^2/4=0.000\,625$ for $L=0$, $\tau_0=h^2/2=0.00\,125$ for $L=1$, and $\tau_0=h^2=0.0025$ for $L=2$.

There is a computational difficulty associated with the use of projective coordinates: namely, in these coordinates the size of bound and single-ionized (bound in one coordinate) states decreases with time, so that the finite-difference approximation finally becomes poor. For the grid parameters used here the ground-state radius becomes smaller than the mesh size long before cross-section convergence is achieved. However, for Coulomb potentials this problem is not essential, because the bound states collapse to the node nearest to the nucleus. This does not affect the double-ionization cross section to which the remote nodes mainly contribute. The probability density integrated over the angular variables versus the radial coordinates of two electrons at $t=t_{int}$ is shown in Figs. 1(a) and 2(a). In Figs. 1(b) and 2(b) the same distribution is shown at large t. The "sidewalls" correspond to single-ionized (SI) states, and the peak near the center corresponds to bound (B) states. The rest smooth part of the distribution corresponds to the double-ionized (DI) state.

More computational problems arise due to doubly excited (autoionization) states. The numerical error increasing with t shifts the real part of the energy of such states. As a result nonphysical oscillations appear in the dependence of the single-ionization cross section upon the energy of the ejected electron (dashed line in Fig. 3). To avoid this artifact we suppress the harmful contributions before starting the coordinate expansion by the following filtration of the initial wave function:

$$\Psi_{flt}^{LM}(t_{int}) = \exp(-\hat{H}_0 t_{flt}) \prod_{n=1}^{N_{flt}} (\hat{H}_0 - E_{Ln}) \Psi^{LM}(t_{int}),$$

where E_{Ln} are the energies of doubly excited states and N_{flt} is the number of doubly excited states significantly excited during the impact. The multiplication by $(\hat{H}_0 - E_{Ln})$ substantially broadens the wave packet in the energy space. To correct it one should suppress the high-energy part of the spectrum by propagating in imaginary time during t_{flt}, which is implemented by the exponential factor. Actually in all our calculations it was enough to take $N_{flt}=1$ and $E_{L1}=-0.625$ with $t_{flt}=0.2$ to make the nonphysical oscillations negligible (solid line in Fig. 3). Evidently, standard methods of noise filtration could be applied with not less efficiency. However, we prefer not only to remove the artifact oscillations, but to reveal and suppress their "physical" source.

The target initial-state function $\psi_0(\mathbf{r}_1, \mathbf{r}_2)$ is found by calculating the propagation in imaginary time [12].

V. RESULTS AND DISCUSSION

In the present work we extend the numerical approach proposed in [15] over the single and double ionization of two-electron targets by fast electrons. As mentioned above, while for $(e,2e)$ and double photoionization the theoretical results agree with the experimental ones, in double ionization by fast-electron impact the disagreements persist [5]. Many attempts have been made to tackle this difficult problem or, at least, to explain the reasons for these disagreements. The first idea was that high-order terms in the Born expansion could be important in this case [6,9], and this can really explain the results for smaller impact electron energy [2], but not for 5.5 keV, when the second-order term of the Born series contributes only by 10% [9]. In some papers an attempt is made to improve the description of the two-electron target initial state by using correlated initial-state functions or even more elaborate functions satisfying the cusp condition [7]. Other attempts aimed to improve the final-state correlation and the description of the double electron continuum [6]. In this state of the art the method developed here approaches the problem from completely different point of view.

To verify our numerical scheme we have first calculated the triple-differential cross section of the ionization of helium by electrons with energy 5600 eV. Figure 4 shows its dependence on the ejection angle for the small scattering angle $\theta_s=0.45°$ and the ejection energy 10 eV. Our results are in very good agreement with the experiment and the first Born CCC calculations with Hylleraas ground state [8].

Figure 5 shows the multifold differential cross section of the double ionization of helium as a function of the ejection angle of one electron at fixed ejection angle of the other electron. Our results are close to those of the CCC method [5] and thus are several times lower in magnitude compared to the experimental results.

Hence, the hypothesis that the disagreement between CCC calculations and experiment is due to the incorrect asymptotic behavior of the CCC two-electron continuum function, which largely stimulated this work, is not verified.

One can see that our results slightly differ from those of the CCC method. To reveal the source of this difference we calculate the double photoionization cross section and compare it with CCC [5,26], HRM-SOW [10], ECS [14], and experimental [25,26] results (Fig. 6). It is clear that our results are closer to those of the ECS method. This fact has minor significance, since the difference mentioned has the order of numerical error.

VI. CONCLUSION

The multiply differential cross section of the double ionization of a helium atom by fast-electron impact is calculated by means of a direct approach, which involves the reduction of the initial nine-dimensional (9D) Schrödinger equation to a 6D evolution problem followed by modeling the wave packet dynamics. This approach allows one to avoid the use of rather cumbersome functions of the continuous spectrum of the two ejected electrons. The evolution problem is reduced to a set of 2D radial matrix equations using the total momentum representation. The numerical method of solving the evolution problem is based on two-step splitting of the repulsive Coulomb interaction between the electrons. To provide an efficient diagonalization of this interaction in the DVR and, thus, to reduce the computational burden considerably, we propose a dynamical version of Chang-Fano transformation. To obtain the cross section versus the ejection energy and angle we used the time-dependent scaling transformation of coordinates.

For simple $(e,2e)$ ionization and double photoionization our results agree with the experimental and CCC results. In case of the $(e,3e)$ double ionization the disagreement persists between the experiment and the theory, including both our results and those of the CCC method. With that, our results are in good agreement with those of the CCC method.

In the next paper we plan to consider the double ionization of He with unequal energy sharing. The computational scheme developed here is clearly applicable to the double photo- and impact ionization of alkaline-earth metals. In future we also plan to develop a scheme based on a modified CF-DVR for the calculation of photoionization and impact ionization excitation and double ionization of molecular hydrogen.

ACKNOWLEDGMENTS

The authors are grateful to Professor Yu. V. Popov, Professor M. Kaschiev, and Professor V. S. Melezhik for useful discussions. This work was supported by Grant No. CRDF BRHE REC-006 SR-006-X1/B75M06 Y3-P-06-08.

[1] A. Lahmam-Bennani, I. Taouil, A. Duguet, M. Lecas, L. Avaldi, and J. Berakdar, Phys. Rev. A **59**, 3548 (1999).
[2] A. Lahmam-Bennani *et al.* J. Phys. B **34**, 3073 (2001).
[3] A. Dorn, A. Kheifets, C. D. Schroter, B. Najjari, C. Hohr, R. Moshammer, and J. Ullrich, Phys. Rev. Lett. **86**, 3755 (2001).
[4] A. Dorn, A. Kheifets, C. D. Schroter, C. Hohr, G. Sakhelashvili, R. Moshammer, J. Lower, and J. Ullrich, Phys. Rev. A **68**, 012715 (2003).
[5] A. S. Kheifets and I. Bray, Phys. Rev. A **69**, 050701(R) (2004).
[6] J. Berakdar, Phys. Rev. Lett. **85**, 4036 (2000).
[7] S. Jones and D. H. Madison, Phys. Rev. Lett. **91**, 073201 (2003).
[8] A. Kheifets, I. Bray, A. Lahmam-Bennani, A. Duguet, and I. Taouil, J. Phys. B **32**, 5047 (1999).
[9] A. S. Kheifets, Phys. Rev. A **69**, 032712 (2004).
[10] P. Selles, L. Malegat, and A. K. Kazansky, Phys. Rev. A **65**, 032711 (2002).
[11] C. W. McCurdy, M. Baertschy, and T. N. Rescigno, J. Phys. B **37**, R137 (2004).
[12] J. Colgan, M. S. Pindzola and F. Robicheaux, J. Phys. B **34**, L457 (2001).
[13] M. Baertschy, T. N. Rescigno, W. A. Isaacs, X. Li, and C. W. McCurdy, Phys. Rev. A **63**, 022712 (2001).
[14] C. W. McCurdy, D. A. Horner, T. N. Rescigno, and F. Martin, Phys. Rev. A **69**, 032707 (2004).
[15] V. V. Serov, V. L. Derbov, B. B. Joulakian, and S. I. Vinitsky, Phys. Rev. A **63**, 062711 (2001).
[16] E. A. Solov'ev and S. I. Vinitsky, J. Phys. B **18**, L557 (1985).
[17] E. Y. Sidky and B. D. Esry, Phys. Rev. Lett. **85**, 5086 (2000).
[18] V. L. Derbov, M. S. Kaschiev, V. V. Serov, A. A. Gusev, and S. I. Vinitsky, Proc. SPIE **5069**, 52 (2003).
[19] A. K. Kazansky, P. Selles, and L. Malegat, Phys. Rev. A **68**, 052701 (2003).
[20] G. I. Marchuk, *Methods of Numerical Mathematics* (Springer-Verlag, New York, 1982).
[21] V. S. Melezhik and D. Baye, Phys. Rev. C **59**, 3232 (1999).
[22] E. S. Chang and U. Fano, Phys. Rev. A **6**, 173 (1972).
[23] N. F. Mott and H. S. W. Massey, *The Theory of Atomic Collisions* (Clarendon, Oxford, 1965), Sec. 2, Chap. 21.
[24] D. A. Varshalovich, A. M. Moskalev, and V. K. Khersonskii, *Quantum Theory of Angular Momentum* (World Scientific, Singapore, 1989).
[25] M. Braüning *et al.*, J. Phys. B **31**, 5149 (1998).
[26] A. Knapp *et al.*, J. Phys. B **38**, 615 (2005).